Journal of Chemical&Engineering Data

pubs.acs.org/jced Article

Evaluating the Effectiveness of Piperazine on Carbon Dioxide Loading in *N*-Methyl Diethanolamine Aqueous Solutions and Water/Oil Microemulsions

Monireh Zolfaghari, Masoud Nasiri,* and Ali Haghighi Asl

Cite This: *J. Chem. Eng. Data* 2024, 69, 1884−1896 Read Online

ACCESS | Metrics & More | Article Recommendations

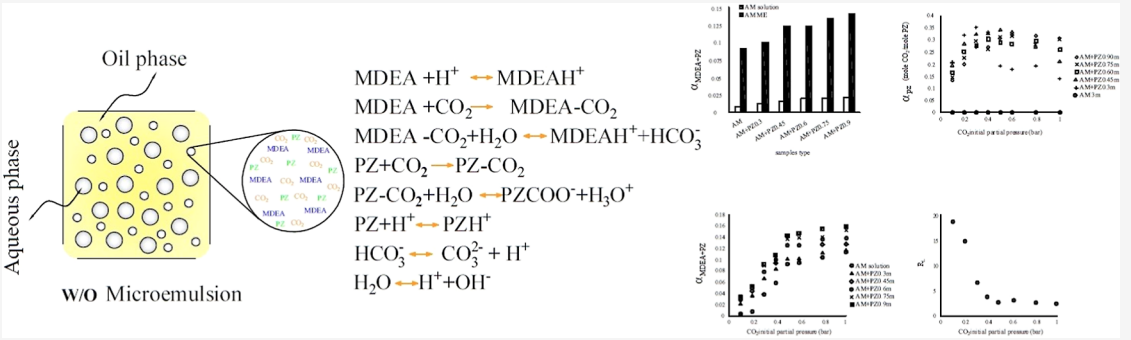

ABSTRACT: This study investigated the chemical absorption of carbon dioxide gas from a carbon dioxide−nitrogen gas mixture at a low partial pressure of carbon dioxide (0.1−1.0 bar) using a water-in-oil microemulsion system. Gas chemisorption in the aqueous phase was examined using *N*-methyldiethanolamine (MDEA) at 3 mol kg^{-1} concentration and piperazine (PZ) at concentrations ranging from 0.3 to 0.9 mol kg^{-1}. The first stage was to assess the effectiveness of the microemulsion system in comparison to that of the nonemulsion system for gas absorption. Then, the aim was to evaluate the effectiveness of PZ in combination with an amine. The results clearly validate the superior gas absorption performance of the microemulsion system compared to that of the nonemulsion system. Furthermore, concerning the effectiveness of PZ, the results indicate that PZ is more efficient at low partial pressures of carbon dioxide than at high pressures. An interesting observation is that in a solution with a constant concentration of MDEA and PZ, as the partial pressure of carbon dioxide gas changes, PZ performs optimally at a partial pressure of 0.3 bar. Additionally, the results obtained confirm the linearity of the relationship between the mole fraction of PZ in the MDEA/PZ solution and the carbon dioxide loading of the MDEA/PZ solution within this pressure range.

INTRODUCTION

Recently, there has been an upward global focus on controlling carbon dioxide emissions and decreasing greenhouse gases in the air.[1,2] Carbon dioxide gas is known as the main source of global warming. Carbon capture and storage (CCS) has emerged as an operational plan to reduce greenhouse gas emissions and mitigate global warming.[3] Among the numerous carbon capture methods, the postcombustion amine process[4,5] stands out as one of the most promising. The amine process, a well-established method, is on the brink of commercialization.[6,7] This technology relies on chemical absorption to remove carbon dioxide from gas streams. It offers numerous advantages including high absorption efficiency, economic viability, ease of operation, and well-established technology. While the chemical absorption method plays a pivotal role in CCS technology, there is a continuous quest to enhance its absorption performance.[8,9]

Chemical absorption of gases in the liquid phase involves a few consecutive steps, which are gas diffusion from the gas phase to the interface between the gas and the liquid, physical dissolution of the gas in the liquid phase, dispersion of the liquefied gas within the liquid bulk, and subsequent chemical reactions between the liquefied gas and a reactant in the liquid phase. The speed of the chemical reaction happens between the reactant in the liquid phase, and the gas is generally fast. However, additional factors, for example, physical suspension within the liquid phase, can influence the gas absorption rate. Increasing the quantity of gas dissolved in the liquid phase can

Received: December 18, 2023
Revised: March 27, 2024
Accepted: March 28, 2024
Published: April 15, 2024

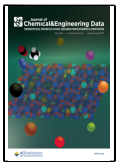

enhance the overall absorption rate, often achieved by maximizing the contact surface area between the gas and liquid phases through the use of small liquid droplets, including emulsions comprising two immiscible liquids.[10] Recent studies have shown a growing interest in gas−liquid structures, such as oil-in-water (o/w) and water-in-oil (w/o) emulsions, for gas absorption.[11−16] Specifically, this study explores microemulsions that are thermodynamically stable and isotropic dispersions of o/w or w/o. Microemulsions are stabilized due to the presence of a surfactant monolayer at the water−oil interface.[17,18] Within this context, this study investigates the experimental capture of carbon dioxide using microemulsions.

While there are widespread reviews on the reactions between carbon dioxide and alkanolamines and the kinetic performance of such reaction systems,[13,19−27] this research focuses on the utilization of alkanolamines, such *N*-methyldiethanolamine (MDEA), for chemical CO_2 absorption.[24,28−30] It is important to note that tertiary alkanolamines, as suggested by Donaldson and Nguyen,[24,31] do not directly react with CO_2. Instead, they catalyze the hydration of the ligands CO_2. It should be noted that the research conducted in the field of investigating the equilibrium solubility of carbon dioxide in amine mixtures containing alkanolamine and piperazine (PZ) is limited. However, relevant work has been conducted in the field of using alkanolamine solutions for carbon dioxide absorption, exemplified by Lensen.[32] Lensen considered the reaction of PZ with MDEA and determined the order of reaction. The results indicated that the addition of PZ to MDEA, combined with temperature elevation, significantly increased the reaction rate constant. This highlights the advantages of utilizing a combination of PZ and MDEA due to the high reaction rate and low reaction enthalpy properties of PZ and MDEA with CO_2, respectively.[32] Zafari and Ghaemi studied the procedure of capturing and reducing CO_2 releases over chemical absorption. They explore the modeling and optimization of the CO_2 mass transfer flux (n_{CO_2}). To achieve this, they employed a mixture of MDEA/PZ amines for CO_2 absorption by the response surface method (RSM). The RSM employs a quadratic model and shows suitable performance in forecasting experimental data.[33] Also, Dugas and Rochelle measured the CO_2 equilibrium partial pressure and liquid film mass transfer coefficient in different concentrations of monoethanolamine (MEA) and PZ in a wet wall column. PZ exhibits a 70% greater CO_2 capacity than MEA, and PZ is shown to absorb CO_2 two to three times faster than MEA.[34] Malekli et al. simulated the absorption system of CO_2 with MDEA/PZ absorbents. In their study, different setups have been considered for designing the absorption tower that has the highest energy consumption to reach the highest absorption, purity, and CO_2 recovery. Energy consumption at a high CO_2 absorption rate and purity is one of the main challenges of such technologies. Finally, they showed that the use of different designs and mixtures can also reduce the required energy costs.[35] PZ is a common component in chemical absorption methods and is often used as an activator in CO_2 absorption solutions rather than as a standalone solvent. Notably, PZ-activated aqueous solutions demonstrate superior CO_2 absorption performance compared to base solutions.[28,30,36] PZ with its cyclical diamine structure containing two secondary amino groups boasts a high CO_2 reaction rate constant. Previous studies have extensively reported on its performance in activated solutions for CO_2 capture, particularly when utilizing membrane methods. Within the realm of alkanolamines, PZ has magnificently contributed to the enhancement of the single alkanol-amine performance. Some research studied stripper (PZAS) technology, which has been well-known as a standard system for amine scrubbing for CO_2 capture from coal-fired flue gas. It has a fast absorption rate, good energy performance, and strong resistance to thermal degradation and oxidation.[37] Freeman measured the density and viscosity of aqueous (PZ + CO_2) solutions over a temperature range of 293.15−333.15 K and concentration ranges of 2−20 mol kg^{-1} PZ and 0−4 mol kg^{-1} CO_2. Data for density and viscosity are offered in a tabular form and contain units valuable for CO_2 capture applications.[38] Esmaeili studied the removal of CO_2 by the blended amine solution of MDEA/PZ with the various molar concentration ratios in a rotating packed bed. The process analysis discovered that rotational speed and PZ concentration have the most important effects on CO_2 absorption efficiency.[39] In general, the combination of MDEA and PZ has been highly regarded due to greater chemical stability and less energy required for solvent renewal.[40] Xu et al. have investigated the influence of PZ on CO_2 loading in MDEA solutions, confirming the usefulness of PZ in enhancing CO_2 loading.[41] Bishnoi et al. investigated the thermodynamics of the MDEA/PZ/CO_2 system. They found that in a solution with 0.6 M PZ and 4 M MDEA at 313 K, the partial pressure of carbon dioxide approaches 1/10th of the value in 4 M MDEA at low loading. This indicates the importance of PZ in the absorption of carbon dioxide in the amine solution.[42,43]

The primary aim of this study is to demonstrate the superior CO_2 absorption capabilities of the MDEA/PZ mixture within a microemulsion structure compared with those in an emulsion structure. Notably, this work considers low partial pressures of carbon dioxide in the feed gas, reflecting real conditions in industrial plants such as power plants, petrochemical units, refineries, and facilities like metal melting and cement factories, where flue gas operates at atmospheric pressure. Additionally, this study assesses the impact of PZ on the rate of absorption of CO_2 into PZ-activated MDEA aqueous solutions across a broader range of PZ concentrations, specifically ranging from 0.3 to 0.9 mol kg^{-1}. The investigation into w/o microemulsions for CO_2 absorption encompasses the evaluation of various parameters, including CO_2 partial pressures, PZ concentration, and microemulsion structure, with a focus on the absorption performance and loading values.

Theoretical Basis. Nowadays, amine-type absorbents are considered suitable solvents for the elimination of carbon dioxide in absorption methods. In the middle of this group of chemical complexes, alkanolamines have received significant consideration in the latest times. Alkanolamines, which have an amine group and a hydroxyl group, are derivatives of ammonia. The amine group can include various subgroups. These different subgroups are defined according to the number of substituents attached to the nitrogen atom. The different classes of alkanolamines include primary, secondary, and tertiary amines with the nitrogen atom attached to one, two, and three substituent groups, respectively. Examples of these classifications include MEA, diethanolamine (DEA), and MDEA.[44] In the process of chemical absorption of CO_2 using a liquid absorbent, CO_2 in the gas phase first dissolves in water and forms carbonic acid (H_2CO_3) in the liquid phase.

Carbonic acid releases a proton and generates a bicarbonate ion (HCO_3^-). The bicarbonate ion, in turn, donates a proton to form a carbonate ion (CO_3^{2-}).[24,45] These reactions are shown in eqs 1−3

https://doi.org/10.1021/acs.jced.3c00750
J. Chem. Eng. Data 2024, 69, 1884−1896

$$CO_2(g) + H_2O \rightleftharpoons H_2CO_3(aq) \quad (1)$$

$$H_2CO_3(aq) \rightleftharpoons HCO_3^-(aq) + H^+(aq) \quad (2)$$

$$HCO_3^-(aq) \rightleftharpoons CO_3^{2-}(aq) + H^+(aq) \quad (3)$$

The reaction that follows between primary or secondary alkanolamines (AM) with CO_2 represents the general reaction that leads to the creation of carbamates,[27] as observed in eq 4

$$2AM(aq) + CO_2(aq) \rightarrow AMH^+(aq) + AMCOO^-(aq) \quad (4)$$

While the reaction that occurs between tertiary alkanolamines with carbon dioxide does not lead to the formation of carbamate types, it would be considered a hydrolysis-catalyzed reaction, as presented in eq 5

$$AM + CO_2 + H_2O \rightleftharpoons AMH^+ + HCO_3^- \quad (5)$$

While primary and secondary alkanolamines exhibit greater reaction rates, tertiary alkanolamines offer greater ability and involve lower heat of renewal.[29] MDEA, being a tertiary amine without a hydrogen atom, requires CO_2 to liquefy in water to produce a bicarbonate ion before undergoing a reaction with the amine, resulting in the overall CO_2 reaction.[46] Tertiary amines like MDEA have the advantage of a theoretical loading capacity of up to 1 mol of CO_2 per mole of amines.[47] MDEA is well-regarded for its low corrosion and degradation rates, allowing for the use of high solution concentrations and making it attractive for CO_2 removal. However, the rate of reaction of the CO_2 with MDEA is slow. To enhance the CO_2 removal process with MDEA, activators such as PZ are added to the aqueous MDEA solution. PZ accelerates the creation of carbamates with CO_2.[28,30,48] A mixture of MDEA and PZ combines the extraordinary capacity of MDEA with the prompt kinetics of PZ.[49] The use of conventional alkanolamines is limited due to their low reaction rates or high heat of renewal. Therefore, incorporating small amounts of primary or secondary type of alkanolamines has become common practice to syndicate the faster reaction rates of primary and secondary type of alkanolamines with lower heat requirements for regeneration and higher stoichiometric loading capacity of tertiary amines in mixed systems. A common example of such a blend used for carbon dioxide removal from industrial gases is an aqueous mixture of PZ-activated MDEA. PZ serves as an effective rate accelerator in such solutions due to its role as a promoter in MDEA.[50]

The following mechanism outlines the series of reactions involving $CO_2(aq)$ with unprotonated/monoprotonated PZ (PZ/PZH^+) and then with the unprotonated/monoprotonated monocarbamates of PZ ($PZCO_2^-/PZCO_2H$)[51] in eqs 6−12

$$PZ + CO_2(aq) \rightleftharpoons PZCO_2H \quad (6)$$

$$PZH^+ + CO_2(aq) \rightleftharpoons PZ(H^+)CO_2H \quad (7)$$

$$PZCO_2^- + CO_2(aq) \rightleftharpoons PZ(CO_2^-)CO_2H \quad (8)$$

$$PZCO_2H + CO_2(aq) \rightleftharpoons PZ(CO_2H)CO_2H \quad (9)$$

$$PZ(H^+)CO_2^- + H^+ \rightleftharpoons PZ(H^+)CO_2H \quad (10)$$

$$PZ(CO_2^-)CO_2^- + H^+ \rightleftharpoons PZ(CO_2^-)CO_2H \quad (11)$$

$$PZ(CO_2^-)CO_2H + H^+ \rightleftharpoons PZ(CO_2H)CO_2H \quad (12)$$

The amine groups presented in the PZ molecule react with CO_2 to yield PZ carbamate and PZ dicarbamate, thereby enhancing the rate of overall CO_2 absorption under operating conditions.[21] Figure 1 illustrates various molecular structures of

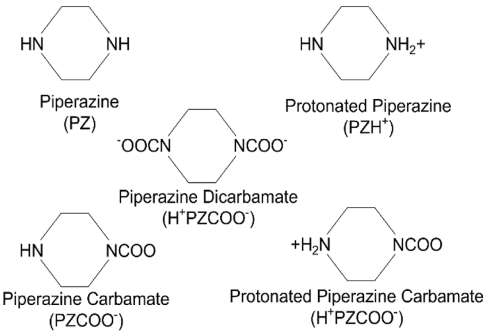

Figure 1. Molecular structures of PZ species.[51]

the PZ species. The main mechanism considered for the reaction of carbon dioxide and MDEA/PZ aqueous solution can be described as a uniform activation mechanism.

The reaction of carbon dioxide and PZ can be assumed to be a fast and pseudo-first-order reaction compared to the reaction of carbon dioxide and MDEA. Since each PZ molecule theoretically has two nitrogen atoms, it can react with 2 mol of carbon dioxide by using stoichiometric relationships. It should be noted that, as reported by Liu et al., the ability of the second amine group to bind the second CO_2 can be neglected.[52] They suggested that in addition to carbamate formation, PZ could also undergo protonation. Thus, even if its concentration is low, effective free PZ can transfer CO_2 to MDEA as a homogeneous activator, significantly enhancing the CO_2 absorption rate in activated MDEA aqueous solutions. During the absorption of CO_2 into aqueous MDEA/PZ solutions, the following reactions can occur[53], as shown in eqs 13−20[13,19,21,54−56]

$$MDEA + H^+ \rightleftharpoons MDEAH^+ \quad (13)$$

$$MDEA + CO_2 \rightleftharpoons MDEA - CO_2 \quad (14)$$

$$MDEA - CO_2 + H_2O \rightleftharpoons MDEAH^+ + HCO_3^- \quad (15)$$

$$PZ + CO_2 \rightarrow PZ - CO_2 \quad (16)$$

$$PZ - CO_2 + H_2O \rightleftharpoons PZCOO^- + H_3O^+ \quad (17)$$

$$PZ + H^+ \rightleftharpoons PZH^+ \quad (18)$$

$$HCO_3^- \rightleftharpoons CO_3^{2-} + H^+ \quad (19)$$

$$H_2O \rightleftharpoons H^+ + OH^- \quad (20)$$

In the MDEA/PZ mixture, the mole fraction values of PZ and MDEA, x_{PZ} and x_{MDEA}, in each solution are determined based on the concentration of PZ and MDEA and can be calculated using the following eq 21

$$x_{MDEA} = \frac{n_{MDEA}}{(n_{MDEA} + n_{PZ})} \qquad x_{PZ} = \frac{n_{PZ}}{(n_{MDEA} + n_{PZ})} \quad (21)$$

where n_{MDEA} and x_{MDEA} and n_{PZ} and x_{PZ} represent the molality and mole fraction of MDEA and PZ, respectively. Additionally, in the Results and Discussion section, we define and present

https://doi.org/10.1021/acs.jced.3c00750
J. Chem. Eng. Data 2024, 69, 1884−1896

Table 1. Chemical Sample Description

chemical name	source	purity (wt %)	CAS	lot no
kerosene	Merck	99	64742-48-9	K49663818-4245
N-methyldiethanolamine	Merck	99	105-459-49	S7114451-4124
piperazine	Merck	99	110-485-40	K47552520-4134
Tween 20	Merck	99	9005-464-45	S8123484-4322
1-butanol	Merck	99.5	71-436-43	K52042890-4109
water	distillated water			
carbon dioxide gas	Tehran Farafan Gas	99.99 mol %		

Table 2. Physical and Chemical Properties of Materials Used

material	molecular formula	molecular weight [g mol^{-1}]	HLB	density [g.cm^{-3}]	CMC [mM]	hydrophobic group[57]	hydrophobic tail [Å]
kerosene	$C_{12}H_{26}$	170		0.82			
N-methyl diethanolamine	$CH_3N(C_2H_4OH)_2$	119.16		1.04			
piperazine	$C_4H_{10}N_2$	86.14		1.1			
Tween 20	$C_{58}H_{114}O_{26}$[58]	1227.54	16.7	1.1	0.0587	Laurate (C_{12})	17
N-butanol	$C_4H_{10}O$	74.121		0.81			

several key parameters including the CO_2 loading of PZ, α_{PZ}, the CO_2 loading of MDEA, α_{MDEA}, the CO_2 total loading, $\alpha_{MDEA/PZ}$, the ratio of α_{PZ} to $\alpha_{MDEA/PZ}$, and finally the ratio of α_{PZ} to α_{MDEA}, R_L. In the gas phase, the ideal gas equation $PV = nRT$ was used to calculate the number of moles of carbon dioxide due to its partial pressure. So, the moles of carbon dioxide in each test could be calculated as $n = \frac{PV}{RT}$, where P is the CO_2 gas pressure, V is the gas phase volume, n is the number of the moles of CO_2 in the gas phase, R is the gas constant, and T is the experimental temperature. It should be noted that the volume of the microemulsion or amine solution was 100 cm^3, and the total volume of the reactor was 600 cm^3, so the volume of the gas was 500 cm^3, which will be explained in the Experimental Section.

All experiments were performed at a temperature of 25 °C and a total pressure of 1 atm. At this temperature, the vapor pressure of water was 0.03085 atm, which is ignored for simplicity in calculations. If the initial partial pressure of carbon dioxide gas in the N_2/CO_2 gas mixture is P_i and reaches equilibrium at a final state pressure of P_{eq}, the pressure difference between the initial and equilibrium states for carbon dioxide gas and the number of moles of CO_2 absorbed by amine solution with ideal gas assumption can be determined from eq 22

$$\Delta P_{CO_2} = P_i - P_{eq}$$
$$n_{abs\ AM}^{CO_2} = \frac{V_g}{RT}\Delta P_{CO_2} \quad (22)$$

where V_g represents the volume of gas. The number of moles of CO_2 chemisorption in the vessel by the MDEA/PZ solution, $n_{abs}^{CO_2}$, is obtained as the difference between the number of initial moles of carbon dioxide gas, $n_i^{CO_2}$, and its number of moles at equilibrium (final state), $n_{eq}^{CO_2}$ assuming an ideal gas by eq 23.

$$n_{abs\ AM}^{CO_2} = n_i^{CO_2} - n_{eq}^{CO_2} \quad (23)$$

Just for simplicity, we will use the symbol $n_{AM}^{CO_2}$ instead of $n_{abs\ AM}^{CO_2}$. CO_2 loading in the liquid phase is defined as eq 24, based on the number of moles of CO_2, which is absorbed in the amine solution, $n_{AM}^{CO_2}$, and the number of moles of amine.

$$\alpha_{AM} = \frac{n_{AM}^{CO_2}}{n_{AM}} \quad (24)$$

where n_{AM} represents the number of moles of amines in the liquid phase. The amine, denoted as AM, can be MDEA, PZ, or their mixture in this research.[30] It has been observed that the relationship between total loading and the mole fraction of PZ is linear when a mass balance is performed in the vessel. The total number of moles of carbon dioxide gas absorbed in the MDEA/PZ solution in the vessel equals the moles absorbed by MDEA plus the moles absorbed by PZ. This relationship can be expressed as eq 25

$$\alpha_{MDEA/PZ} = \alpha_{MDEA} + (\alpha_{PZ} - \alpha_{MDEA})x_{PZ}$$
$$\alpha_{MDEA/PZ} = \frac{n_{MDEA/PZ}^{CO_2}}{n_{MDEA} + n_{PZ}}$$
$$\alpha_{MDEA} = \frac{n_{MDEA}^{CO_2}}{n_{MDEA}}$$
$$\alpha_{PZ} = \frac{n_{PZ}^{CO_2}}{n_{PZ}} \quad (25)$$

where $n_{MDEA/PZ}^{CO_2}$ is the total moles of CO_2 absorbed by n_{MDEA} + n_{PZ} moles of the MDEA/PZ solution, n_{MDEA} and n_{PZ} are the number of moles of MDEA and PZ, and α_{MDEA} and α_{PZ} are the individual CO_2 loading obtained by MDEA and PZ, respectively. The next parameter, R_L, is defined as the ratio of α_{PZ} to α_{MDEA}, and it can be expressed as eq 26. Basically, this parameter determines the degree of effectiveness of PZ in absorbing carbon dioxide next to that of MDEA.

$$R_L = \frac{\alpha_{PZ}}{\alpha_{MDEA}} \quad (26)$$

EXPERIMENTAL SECTION

Materials. Kerosene and MDEA/PZ aqueous solutions were employed as the organic and aqueous phases, respectively. To prepare microemulsions, a nonionic surfactant, commercially known as Tween 20 [polyoxyethylene (20) sorbitan monooleate], was used. Additionally, *n*-butanol alcohol was used as a

https://doi.org/10.1021/acs.jced.3c00750
J. Chem. Eng. Data 2024, 69, 1884−1896

suitable cosurfactant mixed with the surfactant. All materials were sourced from Merck company, and their material properties and molecular structures are provided in Tables 1 and 2.[57,58]

Microemulsion Preparation. The procedure began by weighing a specific amount of Tween 20 and *n*-butanol, ensuring that the surfactant/cosurfactant ratio was maintained at 2. Subsequently, the desired mass of kerosene was added to the mixture. Following this addition, the mixture was subjected to stirring for 15 min at 1000 rpm to achieve complete homogenization. The pre-emulsion was then titrated with a specific quantity of the aqueous phase and stirred for an additional 15 min at 1000 rpm to attain homogeneity. The composition of the w/o microemulsions is detailed in Table 3.

Table 3. Microemulsion Composition Including Oil, Surfactant/Co-surfactant, and Amine Solution

emulsion type	oil phase (% w/w)	surfactants (% w/w)		aqueous phase (% w/w)
		surfactant	cosurfactant	
w/o	18	48	24	10

The rationale behind selecting this combination of materials for synthesizing the microemulsion samples is rooted in the findings presented in Figure 2, specifically, the ternary phase diagram.

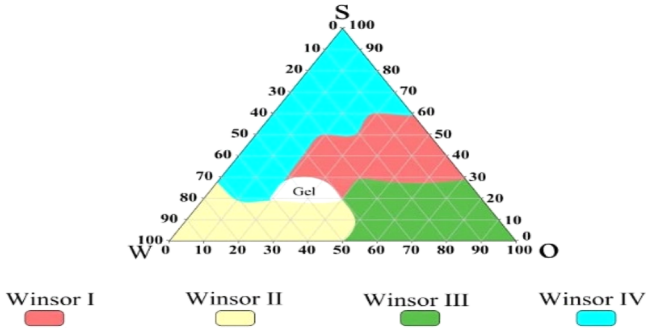

Figure 2. Ternary phase diagram of the kerosene−Tween 20/*n*-butanol−water system (S/C = 2:1).

The chosen material percentages fall within the Winsor IV range indicated in the diagram. It is important to note that w/o microemulsions were favored due to their structural configuration, wherein the internal phase is the aqueous phase. This choice was motivated by the corrosive nature of amine solutions, making it preferable to employ amine solutions as the internal phase, surrounded by the organic phase, thus preventing direct contact with equipment and facilities.

Apparatus. A graphical diagram of the experimental setup employed in this study is illustrated in Figure 3. The central component of the setup comprises a 600 cm^3 Pyrex batch vessel equipped with a pressure transmitter, pH/EC meters, and a thermocouple. Stirring is achieved using a magnetic stirrer. The vessel is outfitted with ports for vacuum, microemulsion sample injection, and gas injection on its upper section. Data loggers connected to a computer system are utilized for analyzing pH and EC data. Additionally, a gas mixture preparation vessel is situated adjacent to the main vessel, equipped with CO_2 and N_2 gas cylinders.

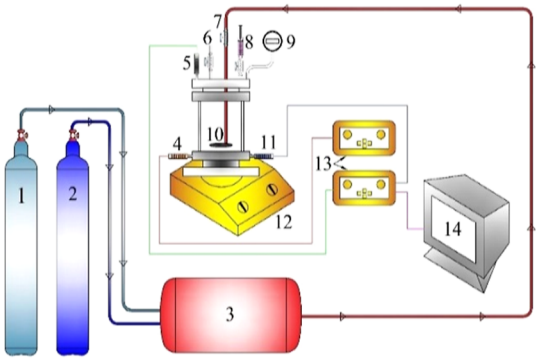

Figure 3. Schematic of the applied setup: (1) CO_2 gas cylinder, (2) N_2 gas cylinder, (3) mixture of gas vessel, (4) EC sensor, (5) temperature sensor, (6) vacuum port, (7) gas inlet port, (8) sample injection port, (9) digital pressure gauge, (10) magnet, (11) pH sensor, (12) digital stirrer, (13) data logger, and (14) computer system.

RESEARCH STRATEGY

First, the inside space of the vessel was evacuated by using a vacuum pump. Subsequently, the microemulsion sample was injected using a syringe. Following this, the adjacent gas vessel was filled with pure nitrogen and pure carbon dioxide from gas cylinders, adjusted according to the desired CO_2 partial pressure. The gas vessel was then connected to the main vessel, allowing gases to flow into it, and injection continued until the total pressure reached 1 bar. This process entailed injecting CO_2 to the desired partial pressure initially and then filling the remaining capacity of the vessel with inert N_2 gas until a total pressure of 1 bar was attained. The system was permitted to achieve an equilibrium between the two phases. The pressure drop indicated carbon dioxide gas absorption. The temperature was maintained at 25 ± 1 °C throughout all absorption tests, and the rotor speed of the stirrer was set at 450 rpm.

RESULTS AND DISCUSSION

Effect of Aqueous Phase Composition on CO_2 Loading. Different compositions of MDEA/PZ solutions were used as the aqueous phase in the w/o microemulsions at various initial partial pressures of CO_2, as presented in Table 4, to investigate their effects on the CO_2 chemical absorption capacity.

Table 4. Aqueous Solutions Used in Terms of MDEA and PZ Concentrations and CO_2 Partial Pressures at 25 °C

MDEA + PZ	concentration (mol kg^{-1})	
MDEA	3	0.1, 0.2, 0.3, 0.4, 0.5, 0.6, 0.8, and 1.0 bar
MDEA + PZ	3 + 0.30	
MDEA + PZ	3 + 0.45	
MDEA + PZ	3 + 0.60	
MDEA + PZ	3 + 0.75	
MDEA + PZ	3 + 0.90	

As mentioned earlier, solutions of MDEA with a concentration of 3 mol kg^{-1} and MDEA/PZ mixtures with different concentrations of PZ were employed as the internal phase in w/o microemulsions for CO_2 absorption. Table 5 presents the carbon dioxide loads measured in terms of carbon dioxide partial

https://doi.org/10.1021/acs.jced.3c00750
J. Chem. Eng. Data 2024, 69, 1884−1896

Table 5. CO_2 Loading in a Microemulsion Containing Blended MDEA/PZ in Terms of the MDEA/PZ Concentration (MDEA 3 mol kg^{-1}, PZ 0.3−0.90 mol kg^{-1}) and CO_2 Partial Pressure (0.1−1 bar) at 25 °C[a]

aqueous phase MDEA: 3 mol kg^{-1}	P_i (bar)	P_{eq} (bar)	$\alpha_{MDEA/PZ}$[b]	α_{PZ}[c]	$\frac{\alpha_{PZ}}{\alpha_{MDEA/PZ}}$	$R_L = \frac{\alpha_{PZ}}{\alpha_{MDEA}}$[d]
PZ: 0 mol kg^{-1}	0.1	0.095	0.0034	0	0	0
	0.2	0.188	0.0080	0	0	0
	0.3	0.243	0.0382	0	0	0
	0.4	0.312	0.0590	0	0	0
	0.5	0.362	0.0925	0	0	0
	0.6	0.459	0.0945	0	0	0
	0.8	0.644	0.1045	0	0	0
	1.0	0.829	0.1146	0	0	0
PZ: 0.30 mol kg^{-1}	0.1	0.064	0.0219	0.2075	9.463	61.939
	0.2	0.140	0.0365	0.3213	8.791	39.961
	0.3	0.190	0.0670	0.3548	5.295	9.290
	0.4	0.262	0.0841	0.3347	3.982	5.677
	0.5	0.333	0.1017	0.1942	1.909	2.100
	0.6	0.432	0.1023	0.1808	1.767	1.914
	0.8	0.615	0.1127	0.1942	1.724	1.858
	1.0	0.808	0.1169	0.1407	1.203	1.228
PZ: 0.45 mol kg^{-1}	0.1	0.051	0.0285	0.1972	6.907	58.860
	0.2	0.124	0.0443	0.2868	6.477	35.671
	0.3	0.170	0.0757	0.3270	4.318	8.563
	0.4	0.238	0.0944	0.3314	3.512	5.621
	0.5	0.285	0.1253	0.3448	2.752	3.729
	0.6	0.384	0.1258	0.3358	2.668	3.555
	0.8	0.582	0.1270	0.2775	2.185	2.655
	1.0	0.781	0.1276	0.2147	1.683	1.874
PZ: 0.60 mol kg^{-1}	0.1	0.045	0.0307	0.1672	5.444	49.902
	0.2	0.112	0.0491	0.2541	5.172	31.605
	0.3	0.160	0.0782	0.2776	3.551	7.268
	0.4	0.221	0.0999	0.3044	3.045	5.162
	0.5	0.275	0.1256	0.2911	2.317	3.148
	0.6	0.374	0.1262	0.2844	2.254	3.010
	0.8	0.555	0.1368	0.2978	2.177	2.849
	1.0	0.751	0.1390	0.2610	1.877	2.278
PZ: 0.75 mol kg^{-1}	0.1	0.04	0.0322	0.1474	4.583	44.000
	0.2	0.103	0.0520	0.2278	4.381	28.333
	0.3	0.132	0.0900	0.2975	3.304	7.789
	0.4	0.214	0.0997	0.2626	2.634	4.445
	0.5	0.245	0.1367	0.3136	2.294	3.391
	0.6	0.340	0.1394	0.3189	2.288	3.376
	0.8	0.538	0.1404	0.2841	2.023	2.718
	1.0	0.715	0.1528	0.3055	2.000	2.667
PZ: 0.90 mol kg^{-1}	0.1	0.035	0.0335	0.1339	3.996	39.961
	0.2	0.098	0.0526	0.2008	3.820	24.976
	0.3	0.121	0.0923	0.2722	2.951	7.128
	0.4	0.190	0.1082	0.2723	2.515	4.618
	0.5	0.223	0.1428	0.3102	2.173	3.355
	0.6	0.315	0.1469	0.3214	2.188	3.402
	0.8	0.501	0.1541	0.3192	2.071	3.054
	1.0	0.691	0.1593	0.3080	1.934	2.688

[a]P_i and P_{eq} are CO_2 initial partial pressure and equilibrium pressure, respectively. Standard uncertainties are $u(T)$ = 1 K; $u(P)$ = 1 kPa; $u(\alpha)$ = 0.0001; and $u(R_L)$ = 0.001. Expanded uncertainty is u(molality) = 0.01 mol kg^{-1} (0.95 level of confidence). [b]Mole ratios of CO_2 to the total amount of amine ($n_{MDEA} + n_{PZ}$). [c]Mole ratios of CO_2 to the amount of piperazine (n_{PZ}). [d]Effectiveness degree.

pressures and the MDEA/PZ concentration in the aqueous phase.

According to the results shown in Table 5, in each solution, the amount of CO_2 loading of PZ, denoted as α_{PZ}, initially increases and then decreases. The optimum loading occurs at a partial pressure of carbon dioxide equal to 0.3 bar. Figure 4 illustrates the ΔP (bar) versus total CO_2 loading diagram for various types of microemulsions synthesized with different concentrations of MDEA/PZ. This figure demonstrates that as the concentration of PZ rises, the amount of CO_2 loading also increases, confirming the positive effect of PZ on carbon dioxide absorption. It should be noted that the graphs drawn in this

https://doi.org/10.1021/acs.jced.3c00750
J. Chem. Eng. Data 2024, 69, 1884−1896

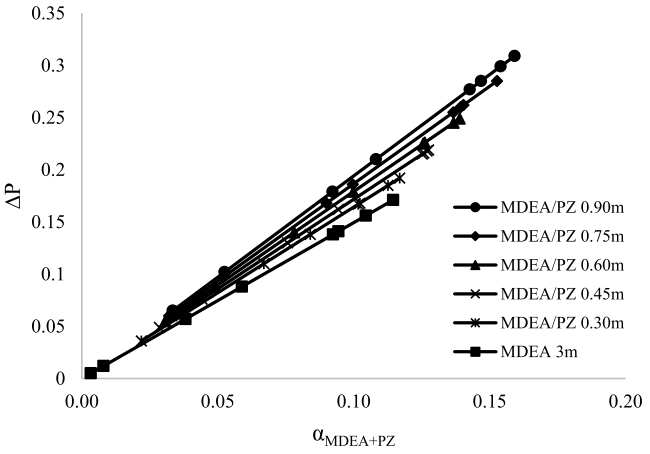

Figure 4. Diagram of pressure differences of CO_2 versus CO_2 loading of MDEA/PZ.

figure are linear since the ideal gas equation was used to determine the number of moles of CO_2 gas absorbed.

Effect of the Mole Fraction of PZ on the CO_2 Total Loading. To explore the influence of PZ on carbon dioxide loading, the results of the experiments are summarized in Table 6. As observed, with a growth in the mole fraction of PZ at a constant pressure, the loading also increases. Similarly, at a fixed mole fraction of PZ in the MDEA/PZ solution, loading increases with higher partial pressures. This is a result of the increased number of moles of carbon dioxide reacting with the MDEA/PZ aqueous phase. Figure 5 illustrates the diagram of the CO_2 total loading in terms of the CO_2 partial pressure in the synthesized microemulsions.

As shown in Figure 6, as the initial partial pressure of carbon dioxide increases, the CO_2 loading of PZ initially rises and then decreases. However, at higher concentrations of PZ, the increase in pressure does not significantly reduce the loading. Consequently, it can be concluded that at higher concentrations of PZ and high pressures, the effect of the PZ concentration becomes insignificant. Figures 6 and 7 are similar, with Figure 7 using the equilibrium pressure (final pressure) on the horizontal axis while maintaining the same trends as in Figure 6. To assess the validity of the relationship described by eq 25, which indicates that CO_2 total loading changes linearly with the PZ mole fraction, we check this against the available data. The correlation coefficient (R-square) of the obtained lines provides acceptable results, which are presented in Table 7. Also, the average absolute deviation (AAD) of a data set is defined as eq 27

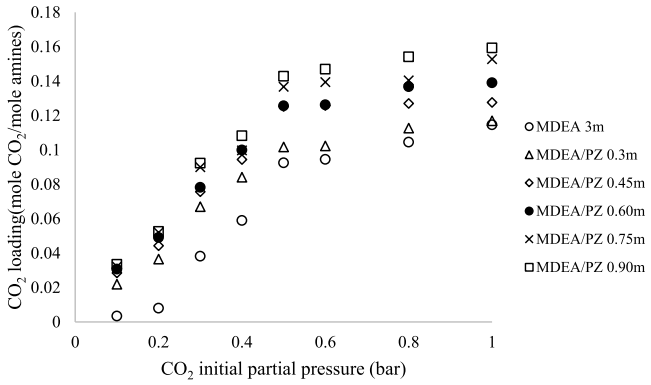

Figure 5. CO_2 total loading versus CO_2 initial partial pressure in MDEA/PZ.

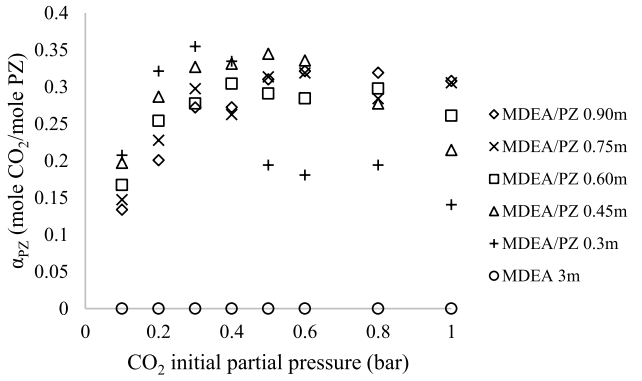

Figure 6. Diagram of the CO_2 loading of PZ, α_{PZ}, versus the initial partial pressure.

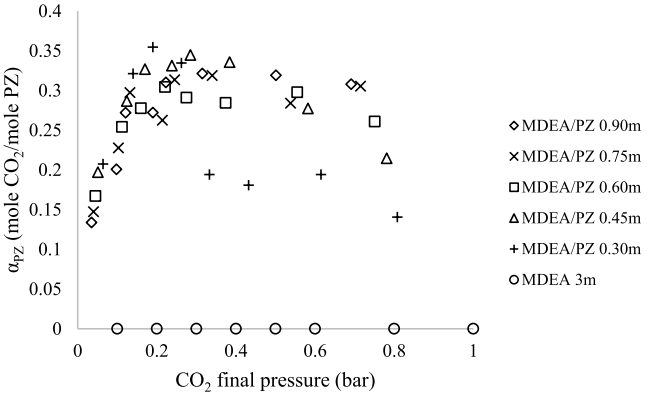

Figure 7. Diagram of the CO_2 loading of PZ, α_{PZ}, versus the final partial pressure.

Table 6. CO_2 Total Loading as a Functional of the Initial Gas Pressure, P_i, and Mole Fraction of PZ, x_{PZ}, at 25 °C in a Microemulsion Containing Blended MDEA/PZ (MDEA 3 mol kg^{-1}, PZ 0.3−0.9 mol kg^{-1}) with the CO_2 Partial Pressure (0.1−1 bar) at 25 °C

x_{PZ}	P_i (bar)							
	0.1	0.2	0.3	0.4	0.5	0.6	0.8	1
0	0.0034	0.008	0.0382	0.0590	0.0925	0.0945	0.1045	0.1146
0.091	0.0219	0.0365	0.0670	0.0841	0.1017	0.1023	0.1127	0.1169
0.130	0.0285	0.0443	0.0757	0.0944	0.1253	0.1258	0.1270	0.1276
0.167	0.0307	0.0491	0.0782	0.0999	0.1256	0.1262	0.1368	0.1390
0.200	0.0322	0.0520	0.0900	0.0997	0.1367	0.1394	0.1404	0.1528
0.231	0.0335	0.0526	0.0923	0.1082	0.1428	0.1469	0.1541	0.1593

https://doi.org/10.1021/acs.jced.3c00750
J. Chem. Eng. Data 2024, 69, 1884−1896

$$\mathrm{AAD} = \frac{1}{N}\sum_{i=1}^{N}\frac{|y_{\mathrm{exp}_i} - y_{\mathrm{cal}_i}|}{y_{\mathrm{exp}_i}} \quad (27)$$

Table 7. Linear Relationship between the CO_2 Total Loading, $\alpha_{MDEA+PZ}$, and x_{PZ}, the Mole Fraction of PZ at a CO_2 Partial Pressure of 0.1−1 bar at 25 °C

P_i (bar)	equation	R^2	AAD
0.1	$\alpha_{MDEA/PZ} = 0.007352 + 0.1297x_{pz}$	0.905	0.0956
0.2	$\alpha_{MDEA/PZ} = 0.01398 + 0.1939x_{pz}$	0.907	0.0873
0.3	$\alpha_{MDEA/PZ} = 0.04187 + 0.2325x_{pz}$	0.967	0.0384
0.4	$\alpha_{MDEA/PZ} = 0.06295 + 0.2049x_{pz}$	0.950	0.0339
0.5	$\alpha_{MDEA/PZ} = 0.0895 + 0.2291x_{pz}$	0.936	0.0325
0.6	$\alpha_{MDEA/PZ} = 0.0902 + 0.237x_{pz}$	0.930	0.0370
0.8	$\alpha_{MDEA/PZ} = 0.1000 + 0.2145x_{pz}$	0.945	0.0243
1	$\alpha_{MDEA/PZ} = 0.1067 + 0.2080x_{pz}$	0.872	0.0396

The values of AAD corresponding to each linear equation are calculated and are given in Table 7. As it is known, the values range from 0.0396 to 0.0956 and indicate that each equation represents the corresponding data well. As seen in Table 7, as the pressure increases, the regression coefficient for the equation representing the loading dependence on the mole fraction of PZ decreases. The equation with the highest regression coefficient was obtained at a pressure of 0.3 bar.

As mentioned earlier, the parameter R_L is defined as the degree of effectiveness, the ratio of α_{PZ} to α_{MDEA}. The results obtained from these equations are presented in Table 8 and Figure 8.

The relationship between R_L and P_i in Figure 8 is given by the following eq 28

$$R_L = \frac{\alpha_{PZ}}{\alpha_{MDEA}} = 16.28\, e^{-55.65P_i^3} + 3.639\, e^{-0.2172P_i^3}$$
$$R^2 = 0.994 \quad (28)$$

According to Table 8 and Figure 8, R_L decreases with a rise in the CO_2 initial partial pressure, confirming that as the partial pressure of carbon dioxide rises, the effectiveness of PZ in CO_2 loading decreases compared to the CO_2 loading of MDEA. This implies that PZ exhibits higher performance at lower partial pressures. The effect of the concentration of PZ at several partial pressures of carbon dioxide is shown in Figure 9a. It is evident that PZ is effective at low pressures, but its effectiveness diminishes with increasing pressure. Figure 9b clearly demonstrates the combined effect of the partial pressure and PZ concentration on gas absorption and its effectiveness. To further investigate the effect of PZ in the MDEA/PZ solution, $\alpha_{PZ}/\alpha_{MDEA+PZ}$ can be calculated. Figure 10 presents $\alpha_{PZ}/\alpha_{MDEA+PZ}$ in terms of the CO_2 equilibrium pressure. It is evident that the effectiveness of PZ is less pronounced at high concentrations, while at lower concentrations, its effectiveness is significant.

Effect of the Microemulsion Structure on CO_2 Loading. To determine the effect of microemulsions on enhancing the absorption capacity, we compared the results with aqueous

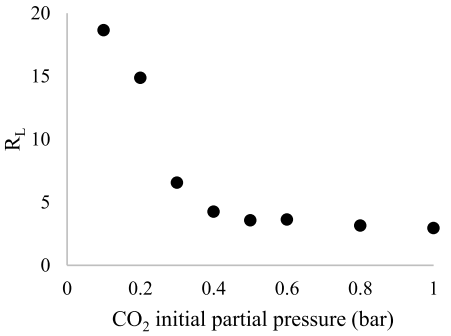

Figure 8. R_L vs CO_2 initial partial pressure diagram.

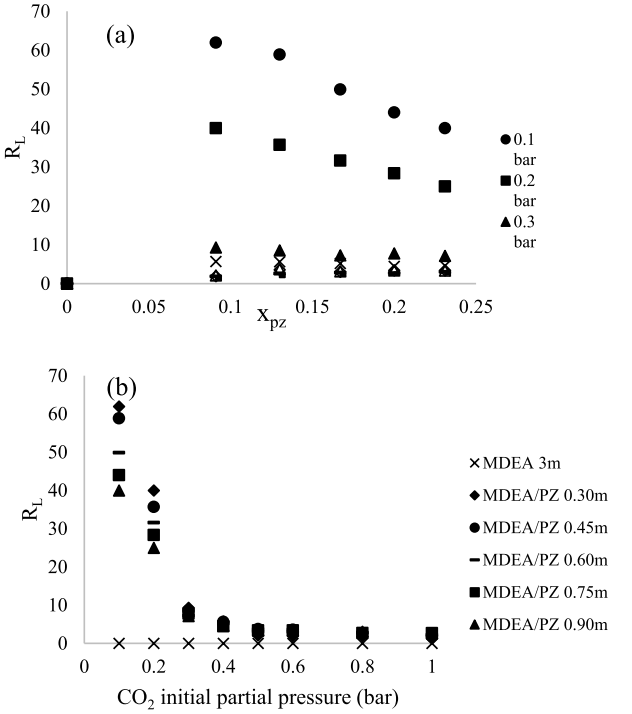

Figure 9. (a) Diagram of R_L versus the molar fraction of PZ at different initial pressures, and (b) diagram of R_L versus CO_2 initial partial pressures in microemulsions with various concentrations of MDEA/PZ.

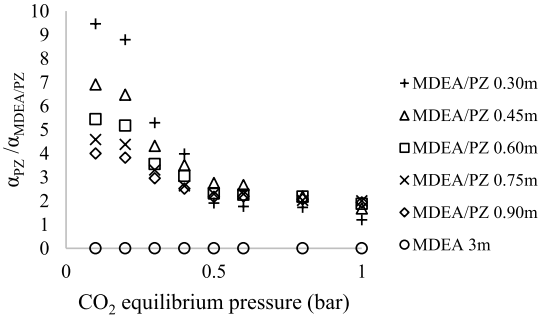

Figure 10. Diagram of the ratio of α_{PZ} to $\alpha_{MDEA/PZ}$ versus CO_2 equilibrium pressure.

Table 8. Effectiveness Degree Values, R_L, for Different P_i, Initial Partial Pressures, at 25 °C

P_i (bar)	0.1	0.2	0.3	0.4	0.5	0.6	0.8	1
R_L	18.641	14.870	6.553	4.255	3.560	3.627	3.145	2.950

https://doi.org/10.1021/acs.jced.3c00750
J. Chem. Eng. Data 2024, 69, 1884−1896

Table 9. Comparison of CO_2 Loading by Amine Solutions and Microemulsions Containing Different Aqueous Phase (MDEA 3 mol kg^{-1}, PZ 0.3−0.90 mol kg^{-1}) and CO_2 Partial Pressure (0.1, 0.3, and 0.5 bar) at 25 °C[a]

pressure (bar)	aqueous phase	$\frac{n_{PZ}}{n_{MDEA}}$	P_{eq} (bar)	$\alpha_{MDEA/PZ}$[b]	α_{PZ}[c]	$\frac{\alpha_{PZ}}{\alpha_{MDEA/PZ}}$	R_L[d]
0.1	MDEA/PZ	0	0.0953	0.0031	0	0	0
	MDEA/PZ ME	0	0.0951	0.0034	0	0	0
	MDEA/PZ + PZ0.3	0.1	0.0925	0.0045	0.0187	4.093	6.032
	MDEA/PZ + PZ0.3 ME	0.1	0.0640	0.0219	0.2075	9.463	61.029
	MDEA/PZ + PZ0.45	0.15	0.0915	0.0049	0.0184	3.715	5.935
	MDEA/PZ + PZ0.45 ME	0.15	0.051	0.0285	0.1972	6.907	58
	MDEA/PZ + PZ0.6	0.2	0.091	0.0050	0.0161	3.203	5.193
	MDEA/PZ + PZ0.6 ME	0.2	0.045	0.0307	0.1672	5.444	49.176
	MDEA/PZ + PZ0.75	0.25	0.090	0.0053	0.0142	2.65	4.580
	MDEA/PZ + PZ0.75 ME	0.25	0.04	0.0322	0.1474	4.583	43.352
	MDEA/PZ + PZ0.9	0.3	0.089	0.0056	0.0140	2.476	4.516
	MDEA/PZ + PZ0.9 ME	0.3	0.035	0.0335	0.1339	3.996	39.382
0.3	MDEA/PZ	0	0.291	0.0054	0	0	0
	MDEA/PZ ME	0	0.243	0.0382	0	0	0
	MDEA/PZ + PZ0.3	0.1	0.283	0.0101	0.0582	5.762	10.777
	MDEA/PZ + PZ0.3 ME	0.1	0.190	0.0670	0.3548	5.295	9.287
	MDEA/PZ + PZ0.45	0.15	0.279	0.0117	0.0542	4.632	10.037
	MDEA/PZ + PZ0.45 ME	0.15	0.170	0.0757	0.3270	4.319	8.560
	MDEA/PZ + PZ0.6	0.2	0.277	0.0126	0.0489	3.880	9.055
	MDEA/PZ + PZ0.6 ME	0.2	0.160	0.0782	0.2776	3.549	7.267
	MDEA/PZ + PZ0.75	0.25	0.274	0.0138	0.0475	3.442	8.796
	MDEA/PZ + PZ0.75 ME	0.25	0.132	0.0900	0.2975	3.305	7.787
	MDEA/PZ + PZ0.9	0.3	0.271	0.0145	0.0452	3.117	8.370
	MDEA/PZ + PZ0.9 ME	0.3	0.121	0.0923	0.2722	2.949	7.125
0.5	MDEA/PZ	0	0.486	0.0092	0	0	0
	MDEA/PZ ME	0	0.362	0.0925	0	0	0
	MDEA/PZ + PZ0.3	0.1	0.478	0.0131	0.0515	3.931	5.597
	MDEA/PZ + PZ0.3 ME	0.1	0.333	0.1017	0.1942	1.909	2.100
	MDEA/PZ + PZ0.45	0.15	0.470	0.0177	0.0739	4.175	8.032
	MDEA/PZ + PZ0.45 ME	0.15	0.285	0.1253	0.3448	2.752	3.727
	MDEA/PZ + PZ0.6	0.2	0.463	0.0204	0.0759	3.720	8.250
	MDEA/PZ + PZ0.6 ME	0.2	0.275	0.1256	0.2911	2.317	3.147
	MDEA/PZ + PZ0.75	0.25	0.461	0.0207	0.0665	3.212	7.228
	MDEA/PZ + PZ0.75 ME	0.25	0.245	0.1367	0.3136	2.294	3.391
	MDEA/PZ + PZ0.9	0.3	0.457	0.0221	0.0649	2.936	7.054
	MDEA/PZ + PZ0.9 ME	0.3	0.223	0.1428	0.3102	2.173	3.353

[a] n_{PZ}, n_{MDEA}, and P_{eq} are number moles of piperazine, MDEA and equilibrium pressure, respectively. Standard uncertainties are $u(T)$ = 1 K; $u(P)$ = 1 kPa; $u(\alpha)$ = 0.0001; and $u(R_L)$ = 0.001. Expanded uncertainty is u(molality) = 0.01 mol kg^{-1} (0.95 level of confidence). [b] Moles ratio of CO_2 to the total amount of amine (n_{MDEA} + n_{PZ}). [c] Moles ratio of CO_2 to the amount of piperazine (n_{PZ}). [d] Effectiveness degree.

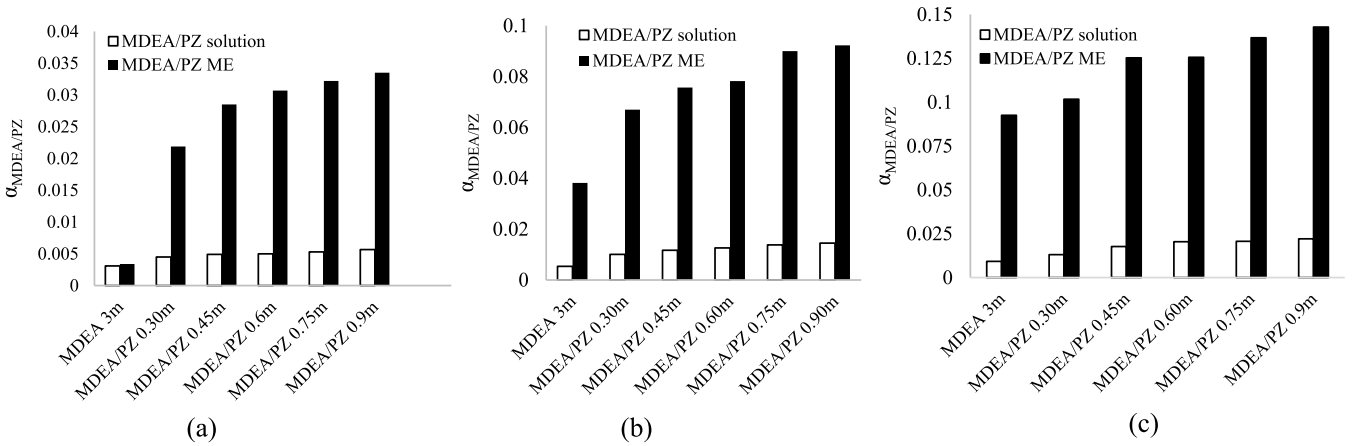

Figure 11. Comparison of the CO_2 loading of the MDEA/PZ solution and microemulsion at (a) 0.1, (b) 0.3, and (c) 0.5 bar CO_2.

https://doi.org/10.1021/acs.jced.3c00750
J. Chem. Eng. Data 2024, 69, 1884−1896

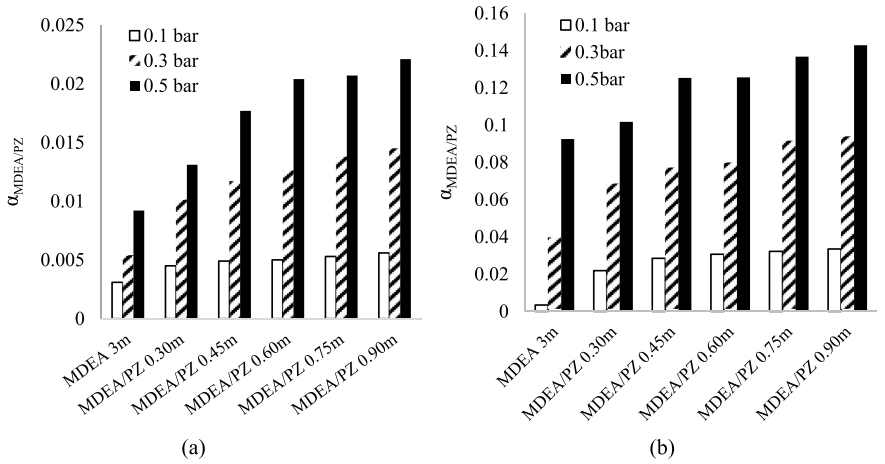

Figure 12. Comparison of the CO_2 loading of (a) MDEA/PZ solution and (b) MDEA/PZ microemulsion at different CO_2 initial partial pressures of 0.1, 0.3, and 0.5 bar.

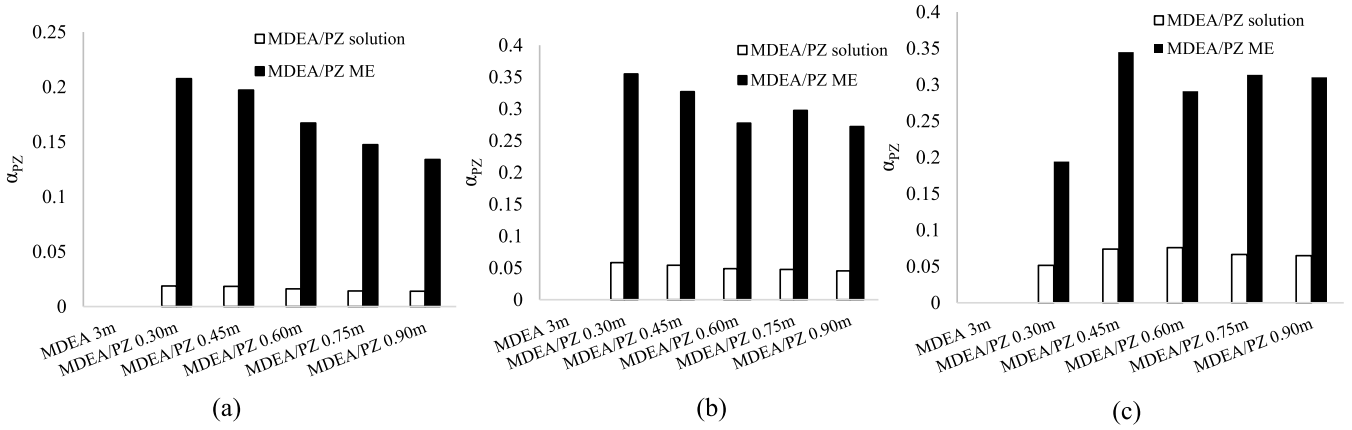

Figure 13. Comparison of the α_{PZ} of the MDEA/PZ solution and the MDEA/PZ microemulsion at (a) 0.1, (b) 0.3, and (c) 0.5 bar CO_2.

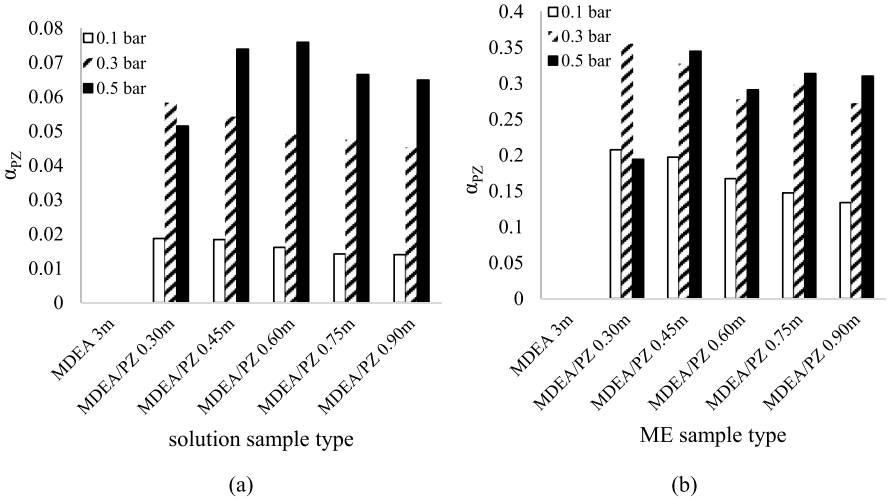

Figure 14. Comparison of the α_{PZ} of (a) the MDEA/PZ solution and (b) the MDEA/PZ microemulsion at different CO_2 initial partial pressures of 0.1, 0.3, and 0.5 bar.

MDEA/PZ samples (without the microemulsion structure). The MDEA/PZ solution, with the same concentration used in the microemulsion structure, was brought into contact with carbon dioxide, and its carbon dioxide loading was calculated at CO_2 partial pressures of 0.1 and 0.5 bar. The results are reported in Table 9 and Figures 11−14.

It is evident that utilizing the MDEA solution in the aqueous phase within the aqueous-phase-in-oil microemulsion structure significantly increases the carbon dioxide absorption capacity. This enhancement is attributed to the presence of aqueous phases in the form of dispersed droplets within the microemulsion structure. Consequently, the contact surface area for

https://doi.org/10.1021/acs.jced.3c00750
J. Chem. Eng. Data 2024, 69, 1884−1896

mass transfer increases, leading to improved absorption capacity compared to that of the pure solution.

Furthermore, upon comparison of the graphs at three different CO_2 initial partial pressures (0.1, 0.3, and 0.5 bar), it becomes apparent that the total loading rate increases with rising pressure. This is because the number of available carbon dioxide moles for absorption increases as the pressure increases.

CONCLUSIONS

In this study, a w/o microemulsion was utilized for the absorption process of carbon dioxide gas. The aqueous phase of this microemulsion consisted of a MDEA/PZ solution, while its oil phase contained kerosene. Throughout all experiments, the concentration of MDEA was maintained at 3 mol kg^{-1}, while the concentration of PZ varied between 0.3 and 0.9. The microemulsion was prepared using Tween 20 as the surfactant and *n*-butanol as the cosurfactant. The prepared microemulsion was introduced into the vessel, and the temperature was held constant at 25 °C. Subsequently, the partial pressure of the gas was adjusted within the range of 0.1−1.0 bar. After equilibrium was reached, CO_2 loading values in the MDEA/PZ solution were measured, and the impact of PZ on gas absorption was calculated. The results of these experiments can be outlined as follows:

Comparing gas absorption in the microemulsion system and the aqueous phase demonstrates that the microemulsion-based absorption method is significantly more efficient. By applying a mass balance for carbon dioxide gas in the vessel, spanning from the initial absorption time to the equilibrium time, it was demonstrated that there is a linear relationship between the mole fraction of PZ and the total loading, as described by eq 25. The results also reveal that the effectiveness of PZ in gas absorption is not constant. At lower pressures, its effectiveness is more pronounced, with the highest loading observed at a partial pressure of 0.3 bar. As the initial gas pressure increases, the total gas absorption also increases, which is expected. However, beyond 0.3 bar, the role of PZ in the absorption process diminishes.

AUTHOR INFORMATION

Corresponding Author

Masoud Nasiri − *Faculty of Chemical, Petroleum and Gas Engineering, Semnan University, Semnan 35131-19111, Iran;* orcid.org/0000-0002-5182-6668; Phone: +982333328860; Email: mnasiri@semnan.ac.ir; Fax: +982333321005

Authors

Monireh Zolfaghari − *Faculty of Chemical, Petroleum and Gas Engineering, Semnan University, Semnan 35131-19111, Iran*

Ali Haghighi Asl − *Faculty of Chemical, Petroleum and Gas Engineering, Semnan University, Semnan 35131-19111, Iran;* orcid.org/0000-0001-9500-4810

Complete contact information is available at: https://pubs.acs.org/10.1021/acs.jced.3c00750

Author Contributions

The manuscript was written through contributions of all authors. All authors have given approval to the final version of the manuscript. These authors contributed equally.

Funding

This work received support from the Iran National Science Foundation and Semnan University Science and Technology Park.

Notes

The authors declare no competing financial interest.

NOMENCLATURE

Symbols

m [mol kg^{-1}]	molality of CO_2 in the aqueous phase
M [mol·L^{-1}]	molarity
n [mol]	number of moles
$n_{AM}^{CO_2}$ [mol]	number of moles of CO_2 absorbed by n_{AM} moles of amine solution
$n_{MDEA/PZ}^{CO_2}$ [mol]	moles of CO_2 absorbed by $n_{MDEA} + n_{PZ}$ moles of MDEA/PZ solution
P_{CO_2} [bar]	partial pressure of CO_2
ΔP_{CO_2} [bar]	pressure difference of CO_2 gas between initial state and equilibrium
R^2 [—]	correlation coefficient
$R_L = \frac{\alpha_{PZ}}{\alpha_{MDEA}}$ [—]	effectiveness degree
T [K]	absolute temperature
x [—]	mole fraction
W [—]	weight fraction

Greek Letters

α	$\left[\frac{\text{the number of moles of absorbed } CO_2}{\text{the number moles of absorbent}}\right]$ CO_2 loading
α_{AM}	$\left[\frac{\text{the number of moles of absorbed } CO_2}{\text{the number moles of amine solution}}\right]$ CO_2 loading of amine solution
α_{MDEA}	$\left[\frac{\text{the number of moles of absorbed } CO_2}{\text{the number of moles of MDEA solution}}\right]$ CO_2 loading of MDEA solution
α_{PZ}	$\left[\frac{\text{the number of moles of absorbed } CO_2}{\text{the number of moles of PZ solution}}\right]$ CO_2 loading of PZ solution
$\alpha_{MDEA/PZ}$	$\left[\frac{\text{the number of moles of absorbed } CO_2}{\text{the number of moles of MDEA / PZ solution}}\right]$ CO_2 loading of MDEA/PZ solution

Subscripts

abs	absorbed
AM	amine solution; *N*-methyldiethanolamine/piperazine
i	initial state
eq	equilibrium state
MDEA	*N*-methyldiethanolamine
PZ	piperazine

REFERENCES

(1) Darde, V.; Van Well, W. J.; Fosboel, P. L.; Stenby, E. H.; Thomsen, K. Experimental measurement and modeling of the rate of absorption of carbon dioxide by aqueous ammonia. *Int. J. Greenhouse Gas Control* **2011**, *5* (5), 1149−1162.

(2) IPCC. Carbon Dioxide Capture and Storage. *IPCC Special Report*; Cambridge University Press: Cambridge, NY, 2005.

(3) Wee, J.-H.; Kim, J.-I.; Song, I. S.; Song, B. Y.; Choi, K. S. Reduction of carbon-dioxide emission applying carbon capture and storage (CCS) technology to power generation and industry sectors in Korea. *J. .Korean Soc. Environ. Eng.* **2008**, *30* (9), 961−972.

(4) Cousins, A.; Wardhaugh, L.; Feron, P. A survey of process flow sheet modifications for energy efficient CO_2 capture from flue gases using chemical absorption. *Int. J. Greenhouse Gas Control* **2011**, *5* (4), 605−619.

(5) Rochelle, G. T. J. S. Amine scrubbing for CO_2 capture. *Science* **2009**, *325* (5948), 1652−1654.
(6) Afkhamipour, M.; Mofarahi, M. Review on the mass transfer performance of CO_2 absorption by amine-based solvents in low-and high-pressure absorption packed columns. *J. RSC Adv.* **2017**, *7* (29), 17857−17872.
(7) Wang, M.; Lawal, A.; Stephenson, P.; Sidders, J.; Ramshaw, C. Post-combustion CO_2 capture with chemical absorption: A state-of-the-art review. *Chem. Eng. Res. Des.* **2011**, *89* (9), 1609−1624.
(8) Peng, Y.; Zhao, B.; Li, L. Advance in post-combustion CO_2 capture with alkaline solution: a brief review. *Energy Procedia* **2012**, *14*, 1515−1522.
(9) Zhang, Z.; Yan, Y.; Zhang, L.; Ju, S. Numerical simulation and analysis of CO_2 removal in a polypropylene hollow fiber membrane contactor. *Int. J. Chem. Eng.* **2014**, *2014*, 1−7.
(10) Mortaheb, H. R.; Asghar Nozaeim, A.; Mafi, M.; Mokhtarani, B. J. C. e. s. Absorption of carbon dioxide in emulsions of aqueous monoethanolamine/diethanolamine solutions in kerosene/n-heptane. *Chem. Eng. Sci.* **2012**, *82*, 44−51.
(11) Gómez-Díaz, D.; Gomes, N.; Teixeira, J. A.; Belo, I. Oxygen mass transfer to emulsions in a bubble column contactor. *J. Chem. Eng.* **2009**, *152* (2−3), 354−360.
(12) Jeon, S. B.; Jung, J. H.; Lee, H. D.; Kim, B. J.; Oh, K. J. Absorption of carbon dioxide in O/W emulsion absorbent: Kinetics of absorption in N-methylcyclohexylamine and 2, 6-dimethylpiperidine emulsion. *Int. J. Greenhouse Gas Control* **2016**, *44*, 1−10.
(13) Kierzkowska-Pawlak, H.; Siemieniec, M.; Chacuk, A. Reaction kinetics of CO_2 in aqueous methyldiethanolamine solutions using the stopped-flow technique. *Chem. Eng. Process.* **2012**, *33* (1), 7−18.
(14) Park, S. W.; Cho, H. B.; Sohn, I. J.; Kumazawa, H. CO2 absorption into w/o emulsion with aqueous amine liquid droplets. *Sep. Sci. Technol.* **2002**, *37* (3), 639−661.
(15) Park, S.-W.; Choi, B.-S.; Lee, B.-D.; Park, D.-W.; Kim, S. Chemical absorption of carbon dioxide with MDEA in a non-Newtonian W/O emulsion. *J. Ind. Eng. Chem.* **2004**, *10* (6), 1033−1042.
(16) Shen, S.; Ma, Y.; Lu, S.; Zhu, C. An unsteady heterogeneous mass transfer model for gas absorption enhanced by dispersed third phase droplets. *Chin. J. Chem.* **2009**, *17* (4), 602−607.
(17) Paul, B. K.; Mitra, R. K. Water solubilization capacity of mixed reverse micelles: effect of surfactant component, the nature of the oil, and electrolyte concentration. *J. Colloid Interface Sci.* **2005**, *288* (1), 261−279.
(18) Stubenrauch, C. *Microemulsions: Background, New Concepts, Applications, Perspectives*; Wiley, 2009.
(19) Barth, D.; Tondre, C.; Delpuech, J. J. Kinetics and mechanisms of the reactions of carbon dioxide with alkanolamines: a discussion concerning the cases of MDEA and DEA. *J. Chem. Eng. Sci.* **1984**, *39* (12), 1753−1757.
(20) Bernhardsen, I. M.; Knuutila, H. K. A review of potential amine solvents for CO_2 absorption process: Absorption capacity, cyclic capacity and pKa. *Int. J. Greenhouse Gas Control* **2017**, *61*, 27−48.
(21) Bishnoi, S.; Rochelle, G. T. Absorption of carbon dioxide into aqueous piperazine: reaction kinetics, mass transfer and solubility. *Chem. Eng. Sci.* **2000**, *55* (22), 5531−5543.
(22) Borhani, T. N. G.; Afkhamipour, M.; Azarpour, A.; Akbari, V.; Emadi, S. H.; Manan, Z. A. Modeling study on CO_2 and H2S simultaneous removal using MDEA solution. *J. Ind. Eng. Chem.* **2016**, *34*, 344−355.
(23) Camacho, F.; Sánchez, S.; Pacheco, R.; La Rubia, M. D.; Sánchez, A. Kinetics of the reaction of pure CO_2 with N-methyldiethanolamine in aqueous solutions. *Int. J. Chem. Kinet.* **2009**, *41* (3), 204−214.
(24) Khan, A. A.; Halder, G.; Saha, A. K. Experimental investigation on efficient carbon dioxide capture using piperazine (PZ) activated aqueous methyldiethanolamine (MDEA) solution in a packed column. *Int. J. Greenhouse Gas Control* **2017**, *64*, 163−173.
(25) Kim, S.; Shi, H.; Lee, J. Y. CO_2 absorption mechanism in amine solvents and enhancement of CO2 capture capability in blended amine solvent. *Int. J. Greenhouse Gas Control* **2016**, *45*, 181−188.
(26) Kruszczak, E.; Kierzkowska-Pawlak, H. CO_2 Capture by Absorption in Activated Aqueous Solutions of N, N-Diethylethanolamine. *Ecol. Chem. Eng. S* **2017**, *24* (2), 239−248.
(27) Kumar, H.; Ravikumar, S. An approach of CO_2 capture technology for mitigating global warming and climate change-an overview. *Recent Advances in Space Technology Services and Climate Change 2010*; IEEE, 2010; pp 364−371.
(28) Edali, M.; Idem, R.; Aboudheir, A. 1D and 2D absorption-rate/kinetic modeling and simulation of carbon dioxide absorption into mixed aqueous solutions of MDEA and PZ in a laminar jet apparatus. *Int. J. Greenhouse Gas Control* **2010**, *4* (2), 143−151.
(29) Vaidya, P. D.; Kenig, E. Y. Acceleration of CO_2 reaction with N, N-diethylethanolamine in aqueous solutions by piperazine. *Ind. Eng. Chem. Res.* **2008**, *47* (1), 34−38.
(30) Zoghi, A. T.; Feyzi, F.; Zarrinpashneh, S. Experimental investigation on the effect of addition of amine activators to aqueous solutions of N-methyldiethanolamine on the rate of carbon dioxide absorption. *Int. J. Greenhouse Gas Control* **2012**, *7*, 12−19.
(31) Donaldson, T. L.; Nguyen, Y. N. Carbon dioxide reaction kinetics and transport in aqueous amine membranes. *Ind. Eng. Chem.* **1980**, *19* (3), 260−266.
(32) Lensen, R. The promoter effect of piperazine on the removal of carbon dioxide. **2004**.
(33) Zafari, P.; Ghaemi, A. Mixed MDEA-PZ amine solutions for CO_2 capture: Modeling and optimization using RSM and ANN approaches. *Case Stud. Chem. Environ. Eng.* **2023**, *8*, 100509.
(34) Dugas, R. E.; Rochelle, G. T. CO_2 absorption rate into concentrated aqueous monoethanolamine and piperazine. *J. Chem. Eng. Data* **2011**, *56* (5), 2187−2195.
(35) Malekli, M.; Aslani, A.; Zolfaghari, Z.; Zahedi, R. CO_2 capture and sequestration from a mixture of direct air and industrial exhaust gases using MDEA/PZ: Optimal design by process integration with organic rankine cycle. *J. Energy. Rep.* **2023**, *9*, 4701−4712.
(36) Zhang, Z.; Chen, F.; Rezakazemi, M.; Zhang, W.; Lu, C.; Chang, H.; Quan, X. Modeling of a CO_2-piperazine-membrane absorption system. *Chem. Eng. Res. Des.* **2018**, *131*, 375−384.
(37) Gao, T.; Rochelle, G. T. CO_2 absorption from gas turbine flue gas by aqueous piperazine with intercooling. *Ind. Eng. Chem. Res.* **2020**, *59* (15), 7174−7181.
(38) Freeman, S. A.; Rochelle, G. T. Density and viscosity of aqueous (piperazine+ carbon dioxide) solutions. *J. Chem. Eng. Data* **2011**, *56* (3), 574−581.
(39) Esmaeili, A.; Tamuzi, A.; Borhani, T. N.; Xiang, Y.; Shao, L. Modeling of carbon dioxide absorption by solution of piperazine and methyldiethanolamine in a rotating packed bed. *Chem. Eng. Sci.* **2022**, *248*, 117118.
(40) Freeman, S. A.; Dugas, R.; Van Wagener, D. H.; Nguyen, T.; Rochelle, G. T. Carbon dioxide capture with concentrated, aqueous piperazine. *Int. J. Greenhouse Gas Control* **2010**, *4* (2), 119−124.
(41) Xu, G.; Zhang, C.; Qin, S.; Wang, Y. Kinetics study on absorption of carbon dioxide into solutions of activated methyldiethanolamine. *Ind. Eng. Chem. Res.* **1992**, *31* (3), 921−927.
(42) Bishnoi, S.; Rochelle, G. T. Thermodynamics of piperazine/methyldiethanolamine/water/carbon dioxide. *Ind. Eng. Chem. Res.* **2002**, *41* (3), 604−612.
(43) Zheng, Y.; El Ahmar, E.; Simond, M.; Ballerat-Busserolles, K.; Zhang, P. CO_2 heat of absorption in aqueous solutions of MDEA and MDEA/piperazine. *J. Chem. Eng. Data* **2020**, *65* (8), 3784−3793.
(44) Penders-van Elk, N. J.; Derks, P. W.; Fradette, S.; Versteeg, G. F. Kinetics of absorption of carbon dioxide in aqueous MDEA solutions with carbonic anhydrase at 298 K. *Int. J. Greenhouse Gas Control* **2012**, *9*, 385−392.
(45) Shim, J. G.; Lee, D. W.; Lee, J. H.; Kwak, N. S. Experimental study on capture of carbon dioxide and production of sodium bicarbonate from sodium hydroxide. *Environ. Eng. Res.* **2016**, *21* (3), 297−303.
(46) Najafloo, A.; Feyzi, F.; Zoghi, A. Modeling solubility of CO_2 in aqueous MDEA solution using electrolyte SAFT-HR EoS. *J. Taiwan. Inst. Chem. Eng.* **2016**, *58*, 381−390.

https://doi.org/10.1021/acs.jced.3c00750
J. Chem. Eng. Data 2024, 69, 1884−1896

(47) Ibrahim, A.; Ashour, F.; Ghallab, A.; Ali, M. Effects of piperazine on carbon dioxide removal from natural gas using aqueous methyl diethanol amine. *J. Nat. Gas. Sci. Eng.* **2014**, *21*, 894−899.
(48) Yu, C. H.; Tan, C. S. Mixed alkanolamines with low regeneration energy for CO_2 capture in a rotating packed bed. *Energy Procedia* **2013**, *37*, 455−460.
(49) Frailie, P. T. Modeling of carbon dioxide absorption/stripping by aqueous methyldiethanolamine/piperazine. Ph.D. Dissertation, The University of Texas at Austin, 2014. http://hdl.handle.net/2152/25019.
(50) Idem, R.; Edali, M.; Aboudheir, A. Kinetics, modeling, and simulation of the experimental kinetics data of carbon dioxide absorption into mixed aqueous solutions of MDEA and PZ using laminar jet apparatus with a numerically solved absorption-rate/kinetic model. *Energy Procedia* **2009**, *1* (1), 1343−1350.
(51) Conway, W.; Fernandes, D.; Beyad, Y.; Burns, R.; Lawrance, G.; Puxty, G.; Maeder, M. Reactions of CO_2 with aqueous piperazine solutions: formation and decomposition of mono-and dicarbamic acids/carbamates of piperazine at 25.0° C. *J. Phys. Chem. A* **2013**, *117* (5), 806−813.
(52) Liu, H. B.; Zhang, C. F.; Xu, G. W. A study on equilibrium solubility for carbon dioxide in methyldiethanolamine− piperazine− water solution. *Ind. Eng. Chem. Res.* **1999**, *38* (10), 4032−4036.
(53) Zhang, X.; Zhang, C. F.; Qin, S. J.; Zheng, Z. S. A kinetics study on the absorption of carbon dioxide into a mixed aqueous solution of methyldiethanolamine and piperazine. *Ind. Eng. Chem. Res.* **2001**, *40* (17), 3785−3791.
(54) Wang, Y.; Zhang, C.; Qin, S. Kinetics study on absorption of carbon dioxide in aqueous MDEA. *J. Chem. Ind. Eng.* **1991**, *4*, 466.
(55) Pagano, J. M.; Goldberg, D. E.; Fernelius, W. C. A thermodynamic study of homopiperazine, piperazine and N-(2-aminoethyl)-piperazine and their complexes with copper (II) ion. *J. Phys. Chem.* **1961**, *65* (6), 1062−1064.
(56) Edwards, T.; Maurer, G.; Newman, J.; Prausnitz, J. M. Vapor-liquid equilibria in multicomponent aqueous solutions of volatile weak electrolytes. *AIChE J.* **1978**, *24* (6), 966−976.
(57) Mandal, A. B.; Gupta, S.; Moulik, S. P. Characterisation of tween 20 & tween 80 micelles in aqueous medium from transport studies. *Indian J. Chem.* **1985**, *24A*, 670−673.
(58) Mehta, S.; Kaur, G.; Bhasin, K. K. Tween-embedded micro-emulsions—Physicochemical and spectroscopic analysis for antitubercular drugs. *AAPS PharmSciTech* **2010**, *11*, 143−153.

https://doi.org/10.1021/acs.jced.3c00750
J. Chem. Eng. Data 2024, 69, 1884−1896